Supplemental Materials and Methods

Primers used in qPCR studies:

Mouse MYH10 F: gggacttgagtgaggagctg

Mouse MYH10 R: gctttgaacctttcgcttg

Mouse PTCH1 F: ctggactctggctccttgtc

Mouse PTCH1 R: caacagtcaccgaagcagaa

Mouse GLI1 F: gaaggaattcgtgtgccatt

Mouse GLI1 R: gcaaccttcttgctcacaca

Mouse GAPDH F: aactttggcattgtggaagg

Mouse GAPDH R: acacattgggggtaggaaca

Western Blots

Samples were boiled in Laemmli buffer for 10 minutes at 95 C. Samples were run on NuPage 4-12% Bis-Tris 1.0mm Mini Protein gels for 90 minutes at 120 V. Proteins were transferred to PVDF via wet transfer for 90 minutes at 32 V. Blots were blocked with 5% non-fat dry milk (NFDM) for 1 hour and then incubated with primary antibodies overnight in 5% NFDM. Blots were washed with TBST for 10 minutes x 3 and then incubated with HRP-conjugated secondary antibodies diluted in 5% NFDM for 1 hour at room temperature. Blots were again washed in TBST for 10 minutes x 3 and then signal was developed using SuperSignal West Femto Maximum Sensitivity Substrate (ThermoFisher) for 5 minutes at room temperature. Each western blot was performed at least N=3 from samples isolated from independent experiments.

Supplemental Table S1. Genetic, demographic, and growth, features of the MYH10 cohort. Demographic information including age, sex, and race/ancestry are presented for each individual. Variant information and inheritance data for the identified *MYH10* variant (NM_001256012.1) is also provided in addition to prior genetic testing and pertinent results. Growth metrics at birth and at last evaluation are also delineated. [a]denotes that the individual is deceased. [b]indicates prenatal demise. Abbreviations: Ind individual, yo years old, mo months old, w weeks gestation, GA gestational age at delivery, Inh inheritance, CMA chromosome microarray, FISH fluorescent *in situ* hybridization, VUS variant of uncertain significance, PW/AS Prader-Willi/Angelman syndrome, SMA spinal muscular atrophy.

Supplemental Table S2. Dysmorphology identified in individuals with heterozygous *MYH10* variants. The reported dysmorphology for each individual is presented by area. [a]denotes that the individual is deceased. [b]indicates prenatal demise. Abbreviations: Ind individual, mo months old, yo years old.

Supplemental Table S3. ACMG/ACP classification of variants identified in the MYH10 cohort. ACMG/ACP criteria are listed in addition to the level of evidence (red, very strong; orange, strong; yellow, medium; green, supporting). Overall variant classification is listed below (VUS, variant of uncertain significance; LP, likely pathogenic; P, pathogenic). Note that these criteria are applied assuming the proposed LOF model for the novel disorder. The variants p.(G734D), p.(E737K), and p.(R740Q) met criterion PM1 based on their close proximity to the critical R740 residue in the motor domain.

Supplemental Figure S1. Full length images of western blot results depicted in the manuscript. (A) Figure S5A. (B) Figure S11A. (C) Figure S11C. (D) Figure S13U. (E) Figure S14D.

Supplemental Figure S2. Variant and phenotypic information of previously published heterozygous *MYH10* variants. (A) Schematic of MYH10 protein structure demarcating the SH3, motor, and myosin tail domains. Variants are mapped to protein structure. (B) Table describing the variant data, inheritance information, phenotypes and gnomAD data for variants identified in the literature. Note that variants 12-15 were excluded from analysis and mapping based on the allele frequency in the gnomAD database. Abbreviations: ASD autism spectrum disorder, ID intellectual disability, GDD global developmental delay, IUGR intrauterine growth restriction, FTT failure to thrive, CDH congenital diaphragmatic hernia, NDD neurodevelopmental disability, AF allele frequency.

Supplemental Figure S3. Computational predictions of the impact of missense variants on *MYH10* using a variety of prediction algorithms. The VarSome tool was used to generate computational predictions using 24 algorithms. Both the score and prediction classification are depicted. The total number of pathogenic/deleterious predictions is depicted below each column.

Supplemental Figure S4. Novel machine learning approaches EVE and VARITY predict pathogenic effects of most identified missense variants. (A) Table describing the overall EVE and VARITY scores for each variant. (B) Heat map generated by EVE at each amino acid affected by missense variants in the cohort. Data is presented for every possible substitution at each locus. The specific variant substitution is bounded with a white box. Color scale with respect to pathogenicity of the EVE score is shown below. (C) Summary of predictions made by

VARITY at each amino acid affected by missense variants in the cohort. Data is provided for each possible substitution at every amino acid. The specific variant substitution is bounded with a yellow box. Gray boxes indicate substitutions that were not tested by the model. Color scale with respect to the pathogenicity of the VARITY score is depicted below.

Supplemental Figure S5. Gene editing strategy and allele confirmation for CAS9-edited *MYH10* knockout cells. (A) DNA sequence of the first exon of *MYH10* shows the location of two different gRNAs (gRNA1 and gRNA2) used to generate the *MYH10*-edited cell lines. The start codon is depicted in bold, the seed sequences of each gRNA are shown in red, and their corresponding protospacer adjacent motifs (PAMs) are shown in green. (B, C) Chromatograms from sequencing of cloned fragments of genomic DNA generated from the *MYH10* exon 1 in lines KO-1 (B) and KO-2 (C). Deleted regions are depicted above each chromatogram. Variant annotation is shown below each chromatogram. Note that all variants are predicted to ultimately produce nonsense/frameshift changes. Allele 2 from line KO-1 (B) and alleles 2 and 3 from KO-2 (C) show two independent editing events present *in cis*. The insertion present in allele 3 of KO-2 (C) does not BLAST to any region of the mouse genome in full nor is it present in any of the vectors used in the gene editing strategy. Note that four alleles are identified in each line that is consistent with the mostly tetraploid state of the NIH/3T3 cells.

Supplemental Figure S6. Validation of CAS9-mediated *MYH10* knockout cells and quantification of acetylated tubulin staining. (A) Western blot of lysates isolated from parental NIH/3T3 cells and various CAS9-edited cell lines and probed with anti-MYH10, anti-MYH9, or anti-β-actin antibodies. Note that a faint band is present in *MYH10* KO cell lines and that this band appears at a lower molecular weight compared to wildtype lines. (B-M) Immunofluorescent analysis of MYH10 protein (red, B-E, J-M) and actin (phalloidin, green, F-M) localization in CAS9-edited NIH/3T3 cell lines. Note the linear, filamentous staining in the

parental NIH/3T3 and WT-1 lines (B, C, J, K) that co-localizes with actin (F, G, J, K) that is reduced and discontinuous in line LOW-1 (D, H, L) and absent in line KO-1 (E, I, M). Nuclei are labeled with DAPI (blue, F-M). Scale bar (B) is 5um. (N-U) Immunofluorescent investigation of primary cilia at 20x using antibodies targeting acetylated tubulin (green, N-U) and ARL13B (red, O, Q, S, U) in NIH/3T3 cells (N, O) and lines WT-1 (P, Q), KO-1 (R, S), and KO-2 (T, U). DAPI labels nuclei (blue, O, Q, S, U). Scale bar (N) is 40um. Note increased intensity of extra-ciliary acetylated tubulin staining. (V) Quantification of whole-field acetylated tubulin fluorescent intensity normalized to DAPI fluorescent intensity between different cell lines. This analysis confirms an increase in acetylated tubulin staining in knockout cell lines compared to controls. Images were quantified using imageJ with 3 fields quantified in each independent experiment performed at least N=3.

Supplemental Figure S7. *MYH10* knockout severely impairs Hedgehog pathway activation downstream of SMO activation and upstream of GLI transcription factor activity. (A, B) qPCR data measuring the relative expression of the HH targets *PTCH1* (A) and *GLI1* (B) in CAS9-edited lines treated with either control- (blue) or NSHH-conditioned media (red). (C-F) HH luciferase assays performed in lines WT-1 and KO-1 and stimulated with either NSHH conditioned media (C), the SMO agonist SAG (D), transfection of a constitutively active SMO construct (SMOM2, E), or expression of the GLI1 transcription factor (F). Cartoons above assays depict the level at which the pathway is being activated. Representative assays are presented that included 2 biologic replicates for each condition and assays repeated N>3.

Supplemental Figure S8. *MYH10* knockdown reduces response to HH pathway activation. (A) qPCR data for *MYH10* expression in NIH/3T3 cells transfected with either control (blue) or *MYH10* siRNA (red) and isolated at 72 and 96 hours post-transfection. (B-C) qPCR data comparing the relative expression of the HH target genes *PTCH1* (B) and *GLI1* (C) in cells

transfected with either control or *MYH10* siRNA and treated with conditioned media isolated from either control transfected cells (PCDNA3) or cells transfected with a construct expressing the secreted and bioactive N-terminal fragment of the SHH ligand (NSHH; red). (D) Hedgehog pathway activity as measured by a HH-responsive luciferase reporter in either control or *MYH10* siRNA transfected NIH/3T3 cells treated with control- (blue) or NSHH-conditioned media (red). Representative assays are shown in each condition, which includes 3 biological replicates and was repeated at least N=3.

Supplemental Figure S9. Gene editing strategy and allele confirmation for CAS9-edited *MYH10* LOW-1 line. (A) DNA sequence of the first exon of *MYH10* shows the location of two different gRNAs (gRNA1 and gRNA2) used to generate the *MYH10*-edited cell lines. The start codon is depicted in bold, the seed sequences of each gRNA are shown in red, and their corresponding protospacer adjacent motifs (PAMs) are shown in green. (B) Chromatograms from sequencing of cloned fragments of genomic DNA generated from the *MYH10* exon 1 in line LOW-1. Deleted regions are depicted above each chromatogram. Variant annotation is shown below each chromatogram. Note that all variants are predicted to ultimately produce nonsense/frameshift changes. A wildtype allele was also isolated from line LOW-1 (data not shown) demonstrating that 3 of 4 *MYH10* alleles have been edited.

Supplemental Figure S10. *MYH10* LOW-1 line shows an intermediate phenotype with respect to primary ciliogenesis, ciliary length control, and Hedgehog pathway activation. (A-I) Immunofluorescent analysis of acetylated tubulin (AcTub, green; A-C, G-I) and ARL13B (red; D-I) in parental NIH/3T3 cells (A, D, G), line LOW-1 (B, E, H), and line KO-2 (C, F, I). Nuclei are stained with DAPI (blue; D-I). Scale bar in A is 5 um. (J) Analysis of the percentage of cells with primary cilia in control and *MYH10*-edited cell lines. Data was collected from 3 random fields of view (>50 cells/field of view) from maximum intensity projections of Z-stack

images. Each experiment repeated at least N=3. (K) Violin plots of ciliary length between control and *MYH10*-edited cell lines. Ciliary length was measured from 100 cilia from maximal intensity projected Z-stacks for each condition and each condition was repeated at least N=3 from independent experiments. (L) Quantification of mean fluorescent intensity of acetylated tubulin staining normalized to DAPI staining in the indicated cell lines. Each condition repeated at least N=3 from independent experiments. (M-N) qPCR data measuring the relative expression of the HH targets *PTCH1* (M) and *GLI1* (N) in CAS9-edited lines treated with either control- (blue) or NSHH-conditioned media (red). Representative assays are presented that included 2 biologic replicates for each condition and assays repeated N>3.

Supplemental Figure S11. A second wildtype line demonstrates normal primary cilia and response to Hedgehog signaling. (A-C) Immunofluorescent analysis of acetylated tubulin (AcTub; green) in parental NIH/3T3 cells (A), line WT-1 (B), and line WT-2 (C). DAPI labels nuclei (blue). Scale bar in A is 5 um. (D) Hedgehog pathway activity as measured by a HH-responsive luciferase reporter in parental NIH/3T3 cells, line WT-1, and line WT-2 that were treated with either DMSO (blue) or SAG (red).

Supplemental Figure S12. MYH10 undergoes proteolytic cleavage when re-expressed in knockout cells and does not rescue Hedgehog signaling. (A) Western blot of lysates isolated from NIH/3T3 cells and line KO-1 transfected with MYH10::HA-pcDNA3 for 24 or 48 hours and probed with an anti-MYH10 and anti-GAPDH antibodies. Note the strong signal from lower molecular weight bands when expressed in line KO-1. (B) HH-luciferase assay comparing control-transfected NIH/3T3 cells and line KO-1 transfected with pcDNA3 or MYH10::HA-pcDNA3 treated with either DMSO (blue) or SAG (red) to activate HH signaling. Representative assays are shown for each condition that includes 2 biologic replicates and repeated at least N=3. (C) Western blot analysis of NIH/3T3 cells transfected with the indicated HA-tagged

MYH10 variants and probed with an anti-HA or anti-GAPDH antibodies. Note most protein is found in the full-length formed with minimal cleavage compared to line KO-1 (A).

Supplemental Figure S13. MYH10 patient variants show normal localization to the actin network. Immunofluorescent analysis of NIH/3T3 cells transiently transfected with the indicated HA-tagged MYH10 variant constructs for 24 hours and stained with anti-MYH10 (red, A and O) or anti-HA (red, B-G, O-U) in addition to phalloidin-488 (green H-U) to label actin. Nuclei are blue (DAPI). Scale bar in (A) 10um.

Supplemental Figure S14. MYH10 patient variant overexpression produces a dominant-negative effect on primary ciliary length. (A) Measurement of mean fluorescent intensity of HA signal by immunofluorescence shows a similar distribution of MYH10 protein overexpression between lines. (B) Violin plots of quantitation of primary ciliary length between NIH/3T3 cell lines stably expressing control (pcDNA3 only), wildtype *MYH10*, p.(G734D), p.(E737K), p.(R740Q), and p.(E1740G). Ciliary length was measured from 100 cilia from maximal intensity projected Z-stacks for each condition and each condition was repeated at least N=3 from independent experiments. (C-T) Representative images of ARL13B (green; C-T) and HA (red; O-T) immunofluorescence in NIH/3T3 stable lines expressing pcDNA3-only (empty vector, C, I, O), wildtype MYH10 (D, J, P), p.(G734D) (E, K, Q), p.(E737K) (F, L, R), p.(R740Q) (G, M, S), and p.(E1740G) (H, N, T). Note that all constructs are HA-tagged to distinguish endogenous vs exogenous protein expression. Nuclei are stained with DAPI (blue; C-T). Panels I-N reflect magnified regions of the boxes outlined in C-H. Scale bar (C) is 10 um. (U) Western blot analysis of HA-expression in monoclonal stable cell lines expressing empty vector (pcDNA3), wildtype *MYH10* (WT), p.(R740Q), and p.(E1740G). GAPDH is used as a loading control.

Supplemental Figure S15. *MYH10* knockout in human RPE-1 cells significantly impacts primary ciliogenesis and ciliary length control. (A) Sequence of exon 1 of human *MYH10*. The gRNA sequence is indicated in red and the corresponding PAM is in red. (B-C) Sequence confirmation of loss-of-function alleles in lines KO-1 (B) and KO-2 (C). (D) Western blot analysis of MYH10 expression in the indicated cell lines. Note that a faint residual band is observed in line KO-1. GAPDH is used as a loading control. (E-P) Immunofluorescent analysis of human RPE-1 cilia labeled with acetylated tubulin (green, E-H) and ARL13B (red, I-P) in parental RPE-1 cells (E, I, M), WT-1 (F, J, N), KO-1 (G, K, O), and KO-2 (H, L, P). DAPI labels nuclei (blue; I-P). Scale bar in J (10 um). (Q) Analysis of the percentage of cells with primary cilia in control and knockout RPE-1 cell lines. (R) Violin plots of ciliary length between control and knockout RPE-1 cell lines. For ciliogenesis quantification, data was collected from 3 random fields of view (>50 cells/field of view) from maximum intensity projections of Z-stack images. Each experiment independently repeated at least N=3. For ciliary length quantitation, 100 cilia were measured from maximal intensity projected Z-stacks for each condition and each experiment was repeated independently at least N=3.

Table S1

Ind#	Age	Sex	Race/ Ancestry	Variant	Inh	Prior testing	Other findings	GA	Birth metrics			Last eval		
									Height	Weight	HC	Height	Weight	HC
1	16mo	F	White	c.2219G>A; p.(Arg740Gln)	*De novo*		None	34w	Z: 2.85	64%ile	47%ile	13%ile	11%ile	56%ile
2	22yo[a]	F	White	c.2219G>A; p.(Arg740Gln)	*De novo*	Karyotype, FISH	46XX,inv(2)(p11.2q13) paternally inherited	42w	41%ile	91%ile	53%ile	19%ile	Z: -5.1	Z: -3.6
3	7yo	F	White	c.111G>T; p.(Trp37Cys)	Maternal	CMA, FISH (7q11.23)	*TAF15* VUS, *de novo*	40w	N/A	44%ile	N/A	57%ile	61%ile	53%ile
4	39yo	F	White	c.111G>T; p.(Trp37Cys)	N/A	None	N/A	N/A	N/A	N/A	N/A	N/A	N/A	N/A
5	17mo	M	White	c.4529_4588dup; p.(Arg1510_Ala1529dup)	*De novo*	CMA, FDG1 and PTPN11 sequencing	None	40w	50%ile	50%ile	75%ile	10%ile	25%ile	90%ile
6	18yo	M	Mexican	c.1183C>A; p.(Leu395Ile) (mosaic)	*De novo*	CMA, Noonan panel	17p13 duplication, VUS (no NDD genes present)	39w	25%ile	50%ile	N/A	1%ile	19%ile	30%ile
7	9yo	M	White	c.2320G>A; p.(Gly774Ser)	*De novo*	CMA, spasticity sequencing panel	None	40w	N/A	N/A	N/A	68%ile	79%ile	80%ile
8	3yo	F	South African, Afrikaans	c.2555G>A; p.(Arg852Gln)	*De novo*	None	None	38w	50%ile	75%ile	75%ile	95%ile	>99%ile	99%ile
9	15yo	F	White	c.2201G>A; p.(Gly734Asp)	*De novo*	CMA, PW/AS studies, sequencing of MECP2, CDKL5, RAI1, and RSK2, metabolic testing	*DDX3X* pathogenic variant, *de novo*	N/A	N/A	N/A	N/A	1%ile	24%ile	20%ile
10	17yo	F	White	c.5219A>G; p.(Glu1740Gly)	*De novo*	None	*FNLA* variant, likely benign, *de novo*	N/A	N/A	N/A	N/A	N/A	N/A	N/A
11	21mo	M	White	c.5519A>G; p.(Lys1840Arg)	*De novo*	Karyotype, CMA	None	37w	5%ile	25%ile	5%ile	3%ile	3%ile	Z: -3
12	14mo	M	Hispanic	c.2554C>T; p.(Arg852Trp)	*De novo*	CMA, fragile X repeat analysis	None	26w	51%ile	76%ile	76%ile	1%ile	1%ile	17%ile
13	23mo	F	White	c.2036 G>A; p.(Gly679Asp)	*De novo*	CMA	None	39w	N/A	72%ile	N/A	77%ile	75%ile	75%ile
14	2yo	F	Indian	c.2209G>A; p.(Glu737Lys)	*De novo*	None	None	37w	33%ile	60%ile	88%ile	3%ile	7%ile	33%ile
15	3yo	M	Arab, White	c.1220_1221del; p.(Leu407Hisfs*33)	*De novo*	CMA, SMA testing	14q32.2 pathogenic deletion (1.1MB), *de novo*	39w	7%ile	1%ile	52%ile	<1%ile	<1%ile	<1%ile
16	34w[b]	M	White	c.2002del; p.(Thr668Glnfs*28)	*De novo*	Karyotype, CMA	Balanced translocation t(1;4)(q31;q28)	N/A	N/A	N/A	N/A	N/A	N/A	N/A

Table S2

Ind#	Age	Sex	Variant	Head/Face	Eyes	Ears	Nose	Mouth/Chin	Extremities
1	16mo	F	c.2219G>A; p.(Arg740Gln)	Prominent forehead	Hypertelorism	Microtia, low-set and posteriorly rotated, pre-auricular pit	Broad and depressed nasal bridge	N/A	Bilateral 5th finger cinodactyly, hypoplastic toe nails
2	22yo[a]	F	c.2219G>A; p.(Arg740Gln)	N/A	Hypertelorism, epiblepharon	Pre-auditory pits	Broad nasal bridge, upturned nasal tip	High palate, supernumerary teeth (8x extractions)	Pes planovalgus, 5th finger brachydactyly, 5th finger clinodactyly
3	7yo	F	c.111G>T; p.(Trp37Cys)	N/A	Hypertelorism	N/A	N/A	N/A	5th finger clinodactyly, curved 3rd/4th toes
4	39yo	F	c.111G>T; p.(Trp37Cys)	N/A	Hypertelorism	N/A	N/A	N/A	N/A
5	17mo	M	c.4529_4588dup60; p.(Arg1510_Ala1529dup)	High forehead, frontal bossinng	Hypertelorism, down-slanting palpebral fissures, ptosis	Low-set (left)	Depressed nasal root, broad nasal bridge, small nose, anteverted nares	N/A	N/A
6	18yo	M	c.1183C>A; p.(Leu395Ile) (mosaic)	Maxillary hypoplasia	Down-slanting palpebral fissures, ptosis	N/A	Large nasal tip, hypoplastic alae, low-hanging columella	Full lips, retrognathia, small and widely spaced teeth	Long thumbs, mildly limited finger extension
7	9yo	M	c.2320G>A; p.(Gly774Ser)	N/A	N/A	Macrotia	N/A	N/A	N/A
8	3yo	F	c.2555G>A; p.(Arg852Gln)	N/A	N/A	N/A	N/A	N/A	N/A
9	15yo	F	c.2201G>A; p.(Gly734Asp)	Coarse facies	Arched eyebrows	N/A	N/A	N/A	Genu valgum (right)
10	17yo	F	c.5219A>G; p.(Glu1740Gly)	N/A	N/A	N/A	N/A	N/A	N/A
11	21mo	M	c.5519A>G; p.(Lys1840Arg)	N/A	N/A	N/A	N/A	N/A	Arthrogryposis
12	14mo	M	c.2554C>T; p.(Arg852Trp)	N/A	N/A	N/A	N/A	N/A	N/A
13	23mo	F	c.2036 G>A; p.(Gly679Asp)	Long narrow face, facial asymmetry (right lower than left)	Hypertelorism, ptosis, long lashes	Notched tragus bilaterally, prominent lobules	N/A	Long philtrum, broad mouth with bow-shaped vermillion, abnormally angled teeth, prominent overbite, thickened palatal ridges	N/A
14	2yo	F	c.2209G>A; p.(Glu737Lys)	Flat, square-shaped occiput	Hypertelorism	Low-set	Broad nasal root and tip	N/A	Broad toes, 5th toe clinodactyly
15	3yo	M	c.1220_1221del; p.(Leu407Hisfs*33)	High forehead	N/A	N/A	N/A	N/A	N/A
16	34wk[b]	M	c.2002del; p.(Thr668Glnfs*28)	N/A	N/A	N/A	N/A	N/A	N/A

Table S3

Description	Evidence	W37C	L395I	G679D	G734D	E737K	R740Q	G774S	R852Q	R852W	E1740G	K1840R	R1510_A1 529dup	L407Hfs*33	T668Qfs*28
Null variant in known LOF gene/disease	PVS1													X	X
Same amino acid change as pathogenic variant	PS1														
De novo	PS2		X	X	X	X	X	X	X	X	X	X	X	X	X
Functional studies supportive	PS3														
Increased prevalence vs controls	PS4														
Mutational hot spot in functional domain	PM1				X	X	X								
Absent from controls	PM2	X	X	X	X	X	X	X	X	X	X	X	X	X	X
Recessive (in trans)	PM3														
Protein length chain changes	PM4												X	X	X
Novel missense change as pathogenic variant	PM5														
Assumed de novo	PM6														
Co-segregation in family	PP1	X													
Missense variant low rate (Z>3.09)	PP2	X	X	X	X	X	X	X	X	X	X	X			
Computational evidence	PP3	X	X	X	X	X	X	X	X	X	X			X	X
Specific phenotype for disease	PP4														
Report of pathogencitiy by lab w/o evidence	PP5														
	Classification	VUS	LP	LP	P	P	P	LP	LP	LP	LP	LP	LP	P	P

Figure S1

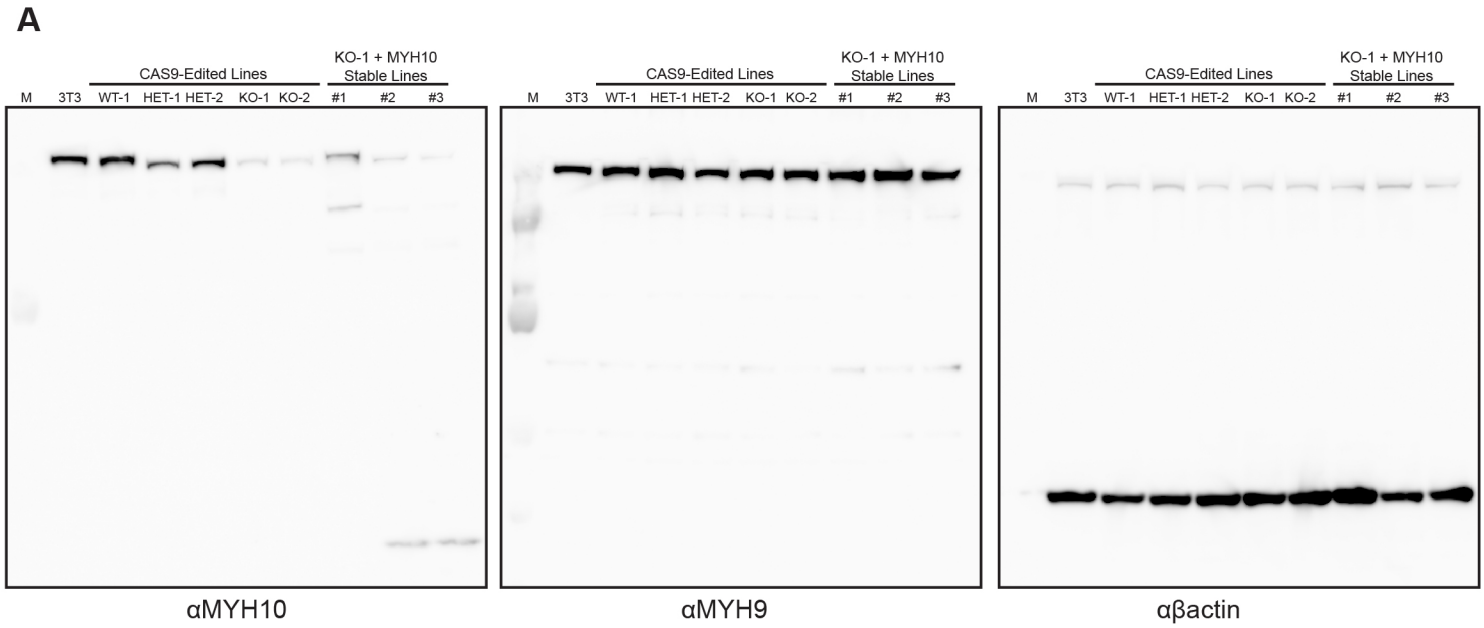
A
CAS9-Edited Lines
KO-1 + MYH10 Stable Lines
M 3T3 WT-1 HET-1 HET-2 KO-1 KO-2 #1 #2 #3
αMYH10
αMYH9
αβactin

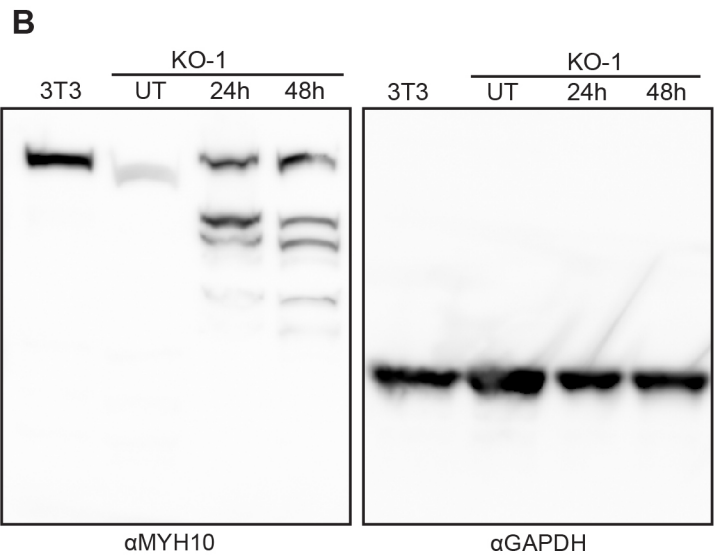
B
KO-1
3T3 UT 24h 48h
αMYH10
αGAPDH

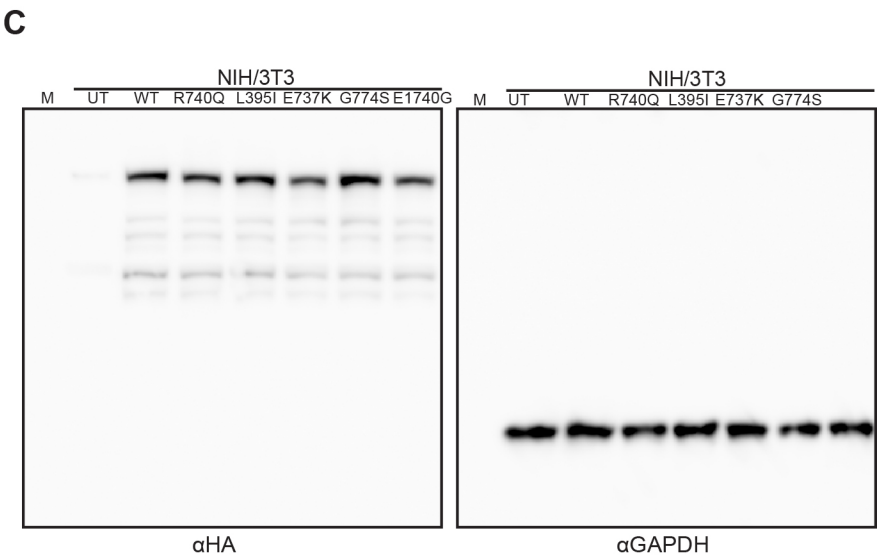
C
NIH/3T3
M UT WT R740Q L395I E737K G774S E1740G
αHA
αGAPDH

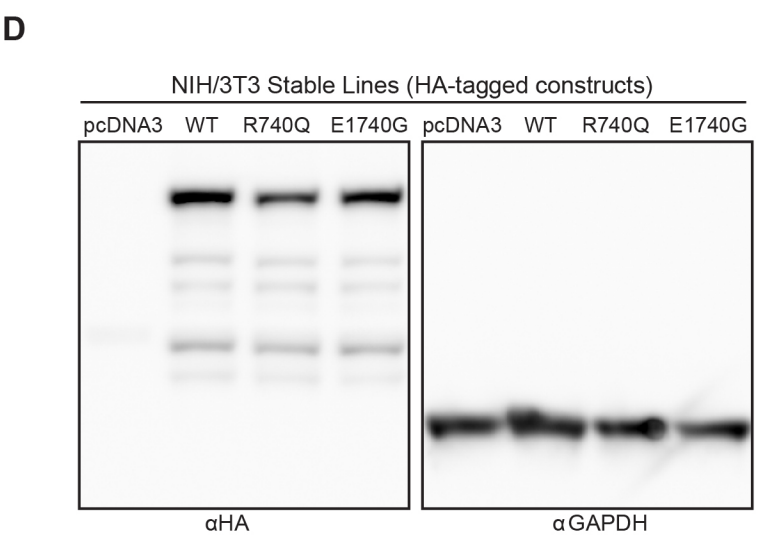
D
NIH/3T3 Stable Lines (HA-tagged constructs)
pcDNA3 WT R740Q E1740G
αHA
αGAPDH

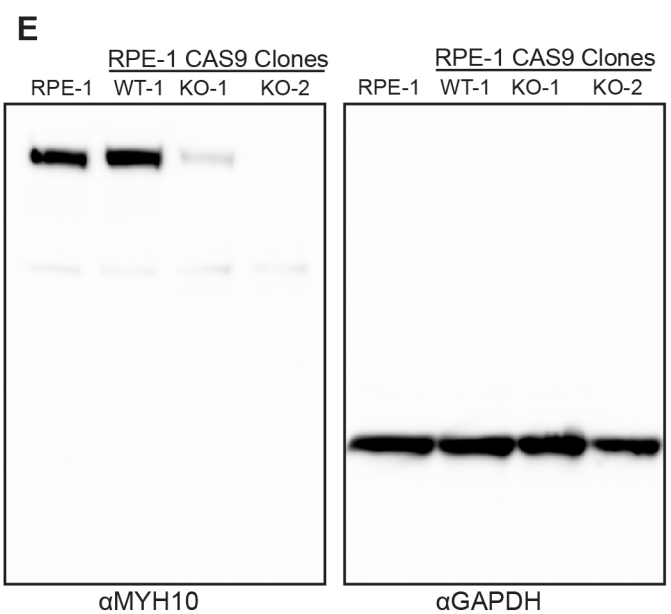
E
RPE-1 CAS9 Clones
RPE-1 WT-1 KO-1 KO-2
αMYH10
αGAPDH

Figure S2

A

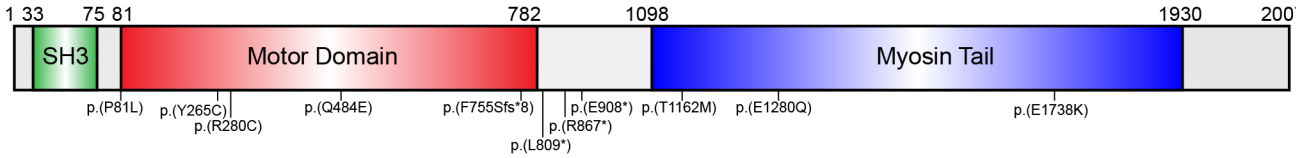

B

#	References	cDNA	Protein	Inheritance	Phenotype	gnomAD		
						Allele count	AF	Homozygotes
1	14, 15, 16	c.242C>T	p.(P81L)	*De novo*	ASD	0	0	0
2	21	c.794A>G	p.(Y265C)	*De novo*	ID	0	0	0
3	13	c.838C>T	p.(R280C)	*De novo*	GDD, ASD, epilepsy, hypotonia, cerebral atrophy, microcephaly, feeding difficulties, aspiration	0	0	0
4	17	c.1450C>G	p.(Q484E)	*De novo*	Schizophrenia	0	0	0
5	14, 15	c.2264delT	p.(F755Sfs*8)	*De novo*	ASD	0	0	0
6	15	c.2426T>G	p.(L809*)	Maternal	ASD	0	0	0
7	11	c.2599C>T	p.(R867*)	*De novo*	Bilateral ventriculomegaly, acqueductal stenosis	0	0	0
8	12	c.2722G>T	p.(E908*)	*De novo*	IUGR, FTT, unilateral multicystic dysplastic kidney, CDH, cryptorchidism, hip dysplasia, severe NDD, hypotonia, cerebral and cerebellar atrophy, hydrocephalus, and microcephaly	0	0	0
9	22	c.3485C>T	p.(T1162M)	*De novo*	CDH	0	0	0
10	20, 22	c.3838C>G	p.(E1280Q)	Paternal	ASD	0	0	0
11	20	N/A	p.(E1738K)	*In trans* (Homozygous)	Dysplastic tricuspid valve, pulmonary atresia, unspecified extracardiac manifestations	0	0	0
12	18	c.4714G>A	p.(V1572M)	N/A	ASD	43/282834	1.52e-4	0
13	16	c.2987C>T	p.(A996V)	Paternal	ASD	2476/281066	8.81e-3	19
14	16	c.4672-34C>T	Intronic	*De novo*	ASD	6/247782	2.42e-5	0
15	15, 16	c.4672-33G>A	Intronic	*De novo*	ASD	14/279368	5.01e-5	0

Figure S3

	p.(W37C)		p.(L395I)		p.(G679D)		p.(G734D)		p.(E737K)		p.(R740Q)	
	Prediction	Score	Prediction	Score	Prediction	Score	Prediction	Score	Prediction	Score	Prediction	Score
BayesDel addAF	Damaging	0.535	Damaging	0.2565	Damaging	0..3497	Damaging	0.5762	Damaging	0.4397	Damaging	0.3928
BayesDel noAF	Damaging	0.5307	Damaging	0.1306	Damaging	0.2645	Damaging	0.5898	Damaging	0.3938	Damaging	0.3263
DANN	N/A	0.9929		0.9925		0.9987		0.9984		0.9994		0.9995
DEOGEN2	Damaging	0.8439	Damaging	0.6801	Damaging	0.8174	Damaging	0.9518	Damaging	0.9453	Damaging	0.8114
EIGEN	Pathogenic	0.9862	Pathogenic	0.5757	Pathogenic	0.9934	Pathogenic	0.9878	Pathogenic	1.0301	Pathogenic	0.8135
EIGEN PC	Pathogenic	0.8845	Pathogenic	0.5593	Pathogenic	0.9519	Pathogenic	0.8029	Pathogenic	0.9339	Pathogenic	0.6636
FATHMM	Damaging	-3.34	Damaging	-2.87	Damaging	-2.22	Damaging	-5.07	Tolerated	-1.36	Tolerated	-1.07
FATHMM-MKL	Damaging	0.9867	Damaging	0.9459	Damaging	0.986	Damaging	0.9831	Damaging	0.9831	Damaging	0.975
FATHMM-XF	Damaging	0.9415	Damaging	0.5371	Damaging	0.9296	Damaging	0.9054	Damaging	0.9046	Damaging	0.8673
LIST-S2	Damaging	0.9922	Damaging	0.9519	Damaging	0.9846	Damaging	0.9963	Damaging	0.9972	Damaging	0.9976
LRT	Deleterious	0	Deleterious	0	Deleterious	0..3497	Deleterious	0	Deleterious	0	Deleterious	0
M-CAP	Damaging	0.5972	Damaging	0.06271	Damaging	0.141	Damaging	0.7709	Damaging	0.5065	Damaging	0.2667
MVP	Pathogenic	0.9842	Benign	0.8925	Pathogenic	0.9258	Pathogenic	0.9899	Pathogenic	0.9584	Pathogenic	0.9697
MetaLR	Damaging	0.9331	Damaging	0.7749	Damaging	0.8429	Damaging	0.9873	Damaging	0.9063	Damaging	0.9012
MetaRNN	Damaging	0.9573	Damaging	0.6606	Damaging	0.8406	Damaging	0.9918	Damaging	0.9886	Damaging	0.9847
MetaSVM	Damaging	1.0909	Damaging	0.6672	Damaging	0.8325	Damaging	0.9769	Damaging	1.0519	Damaging	1.0336
MutPred	Pathogenic	0.738	Pathogenic	0.675	Pathogenic	0.55	Pathogenic	0.946	Pathogenic	0.937	Pathogenic	0.96
Mutation assessor	High	3.875	Medium	3.055	Medium	2.865	High	4.2	High	3.665	Medium	2.77
MutationTaster	Disease causing	1	Disease causing	0.9999	Disease causing	1	Disease causing	1	Disease causing	1	Disease causing	0.9999
PROVEAN	Damaging	-12.62	Neutral	N/A	Damaging	-6.88	Damaging	-6.88	Damaging	-3.86	Damaging	-3.86
PrimateAI	Damaging	0.8726	Damaging	0.8259	Damaging	0.93	Damaging	0.9353	Damaging	0.9122	Damaging	0.867
REVEL	Pathogenic	0.925	Pathogenic	0.6819	Pathogenic	0.8159	Pathogenic	0.9599	Pathogenic	0.948	Pathogenic	0.785
SIFT	Damaging	0	Damaging	0.003	Damaging	0.001	Damaging	0	Damaging	0	Damaging	0
SIFT4G	Damaging	0	Damaging	0.014	Damaging	0.001	Damaging	0.001	Damaging	0.003	Damaging	0.003
		24/24		22/24		24/24		24/24		23/24		23/24

	p.(G774S)		p.(R852Q)		p.(R852W)		p.(E1740G)		p.(K1840R)	
	Prediction	Score	Prediction	Score	Prediction	Score	Prediction	Score	Prediction	Score
BayesDel addAF	Damaging	0.2414	Damaging	0.2546	Damaging	0.2193	Damaging	0.3931	Tolerated	0.05974
BayesDel noAF	Damaging	0.109	Damaging	0.1279	Damaging	0.07732	Damaging	0.3268	Tolerated	-0.1519
DANN		0.9987		0.9996		0.9993		0.9989		0.9757
DEOGEN2	Damaging	0.7188	Damaging	0.6839	Damaging	0.7491	Damaging	0.8077	Tolerated	0.1645
EIGEN	Pathogenic	0.5234	Pathogenic	0.9219	Pathogenic	0.4579	Pathogenic	0.7409	Benign	0.007961
EIGEN PC	Pathogenic	0.5496	Pathogenic	0.88372	Pathogenic	0.3757	Pathogenic	0.6185	Benign	0.2043
FATHMM	Tolerated	-0.53	Tolerated	2.23	Tolerated	2.12	Damaging	-1.66	Tolerated	-1.2
FATHMM-MKL	Damaging	0.9908	Damaging	0.9915	Damaging	0.9493	Damaging	0.9829	Damaging	0.9794
FATHMM-XF	Damaging	0.9098	Damaging	0.9152	Damaging	0.7761	Damaging	0.9366	Damaging	0.7736
LIST-S2	Damaging	0.9619	Damaging	0.9931	Damaging	0.9789	Damaging	0.9602	Damaging	0.8959
LRT	Deleterious	0	Deleterious	0	Deleterious	0	Deleterious	0	Deleterious	1.00E-006
M-CAP	Damaging	0.1007	Tolerated	0.02307	Tolerated	0.02362	Damaging	0.2979	Tolerated	0.01144
MVP	Benign	0.8167	Benign	0.8373	Benign	0.8995	Benign	0.8454	Benign	0.8183
MetaLR	Damaging	0.6717	Tolerated	0.1824	Tolerated	0.1293	Damaging	0.7643	Tolerated	0.2949
MetaRNN	Damaging	0.6198	Damaging	0.7929	Damaging	0.8505	Damaging	0.9086	Tolerated	0.4045
MetaSVM	Damaging	0.034	Tolerated	-0.6469	Tolerated	-0.9746	Damaging	0.7452	Tolerated	-0.5431
MutPred	Benign	0.445	N/A	N/A	Pathogenic	0.627	Pathogenic	0.61	Benign	0.33
Mutation assessor	Low	1.075	Medium	3.245	Medium	1.985	High	3.885	Low	0.805
MutationTaster	Disease causing	1	Disease causing	1	Disease causing	0.9999	Disease causing	1	Disease causing	1
PROVEAN	Damaging	-5.83	Damaging	-3.66	Damaging	-7.32	Damaging	0.8529	Tolerated	0.7369
PrimateAI	Damaging	0.9171	Damaging	0.8733	Damaging	0.9223	Tolerated	0.76	Tolerated	0.7369
REVEL	Benign	0.6069	Benign	0.4289	Benign	0.4259	Pathogenic	0.8529	Benign	0.3429
SIFT	Tolerated	0.141	Damaging	0.003	Tolerated	0.109	Damaging	0	Tolerated	1
SIFT4G	Tolerated	0.323	Damaging	0.017	Tolerated	0.1	Damaging	0.001	Tolerated	0.877
		17/24		17/23		16/24		22/24		5/24

Figure S4

A

Variant	EVE Score	EVE Class (75%)	VARITY_R	VARITY_ER
p.(W37C)	0.977	Pathogenic	0.966	0.89
p.(L395I)	0.51	Uncertain	0.594	0.289
p.(G679D)	0.856	Pathogenic	0.908	0.944
p.(G734D)	0.979	Pathogenic	0.961	0.908
p.(E737K)	0.991	Pathogenic	0.931	0.81
p.(R740Q)	0.972	Pathogenic	0.802	0.616
p.(G774S)	0.461	Uncertain	0.832	0.696
p.(R852Q)	0.662	Pathogenic	0.816	0.654
p.(R852W)	0.792	Pathogenic	0.825	0.737
p.(E1740G)	0.869	Pathogenic	0.805	0.745
p.(K1840R)	0.0942	Benign	0.105	0.117

B

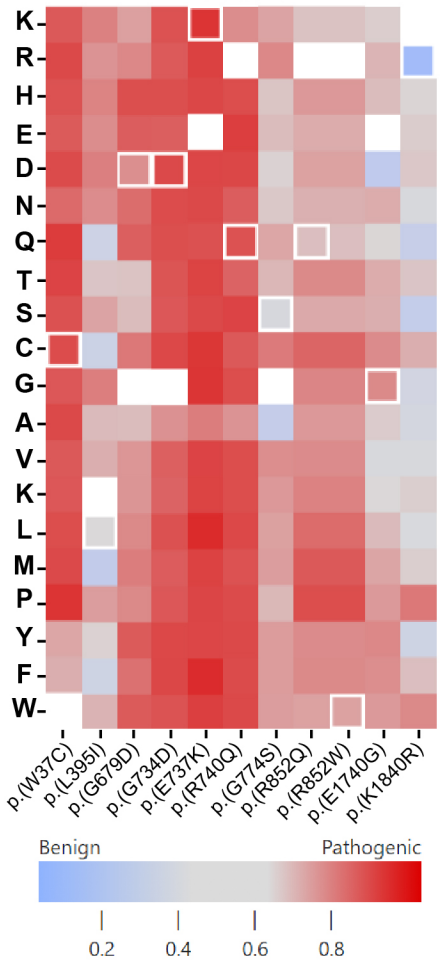

C

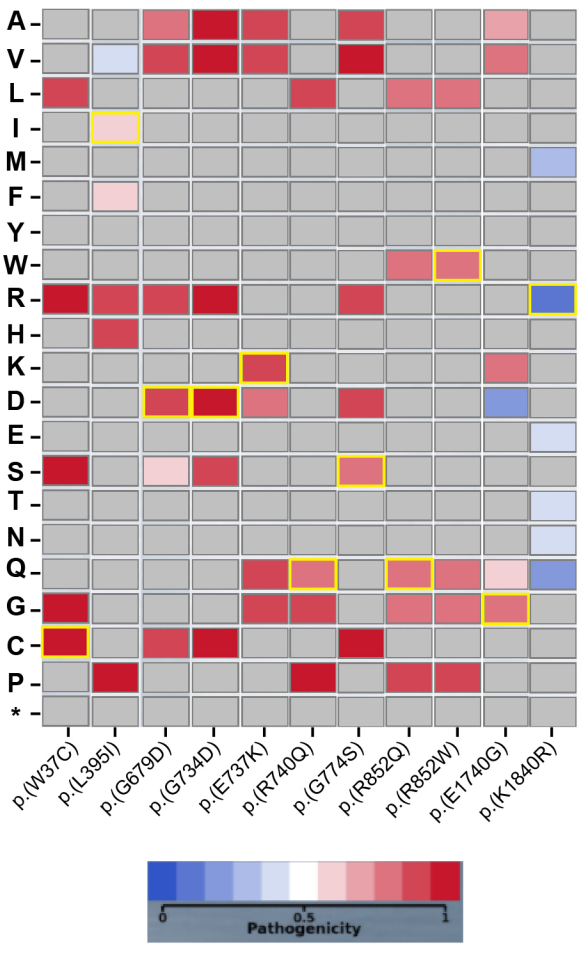

Figure S5

A

Exon 1 (mouse NIH/3T3)

```
1   ATGGCCCAGAGAACTGGACTGGAGGATCCCGAGAGGTATCTCTTTGTGGACAGGGCTGTCATCTACAACCCTGCCACTCAAGCTGACTGGACAGCTAAAAAGCTGGTGTGGATTC   115

116 CATCGGAACGCCATGGTTTTGAGGCAGCTAGTATTAAAGAAGAGCGGGGCGATGAGGTTATGGTGGAGCTGGCAGAGAATGGGAAGAAAGCAATGGTCAACAAAGATGACATTCA   230
                            gRNA1

231 GAAGATGAACCCACCAAAGTTCTCCAAGGTGGAGGATATGGCAGAGCTGACATGCTTGAACGAAGCCTCTGTCTTACATAATTTGAAGGACCGCTACTATTCAGGACTTATCTAT   345
                gRNA2
```

B

Line: KO-1

Allele #1

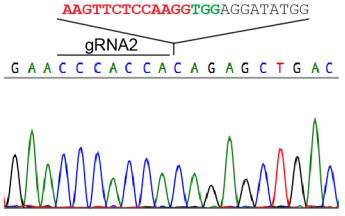

c.247_271del; p.(Lys81GlnfsX2)

Allele #2 (both variants *in cis*)

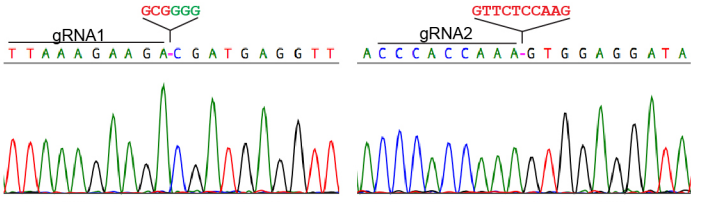

c.159_165del; p.Glu53_Arg54delinsAsp

c.249_259del; p.Phe84_TrpfsX6

Allele #3

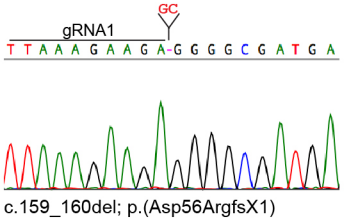

c.159_160del; p.(Asp56ArgfsX1)

Allele #4

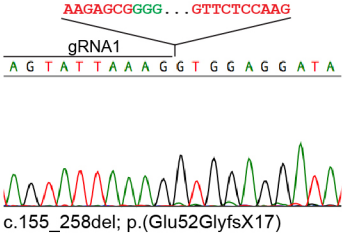

c.155_258del; p.(Glu52GlyfsX17)

C

Line: KO-2

Allele #1

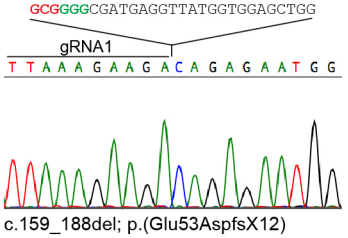

c.159_188del; p.(Glu53AspfsX12)

Allele #2 (both variants *in cis*)

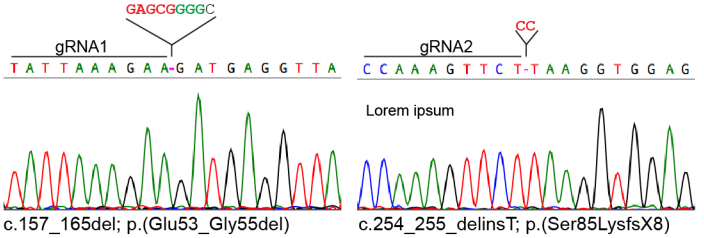

c.157_165del; p.(Glu53_Gly55del)

c.254_255_delinsT; p.(Ser85LysfsX8)

Allele #3 (both variants *in cis*)

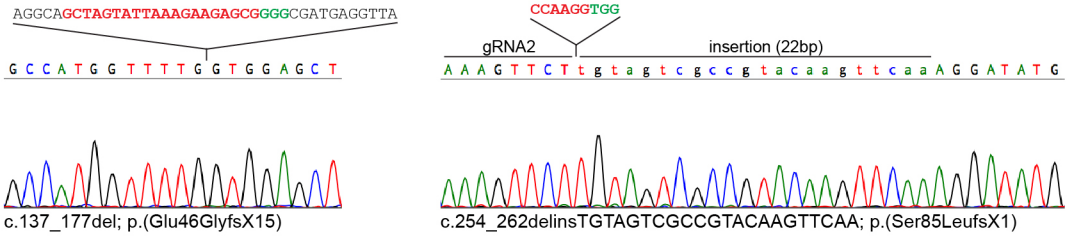

c.137_177del; p.(Glu46GlyfsX15)

c.254_262delinsTGTAGTCGCCGTACAAGTTCAA; p.(Ser85LeufsX1)

Allele #4

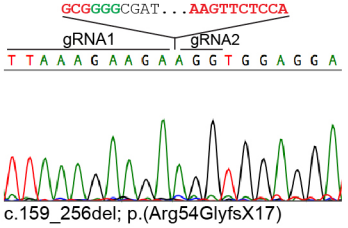

c.159_256del; p.(Arg54GlyfsX17)

Figure S6

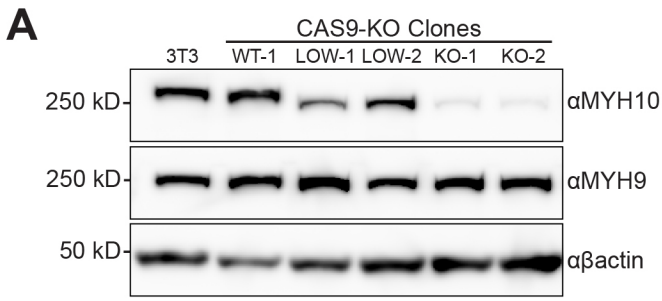
A
CAS9-KO Clones
3T3
WT-1
LOW-1
LOW-2
KO-1
KO-2
250 kD
αMYH10
250 kD
αMYH9
50 kD
αβactin

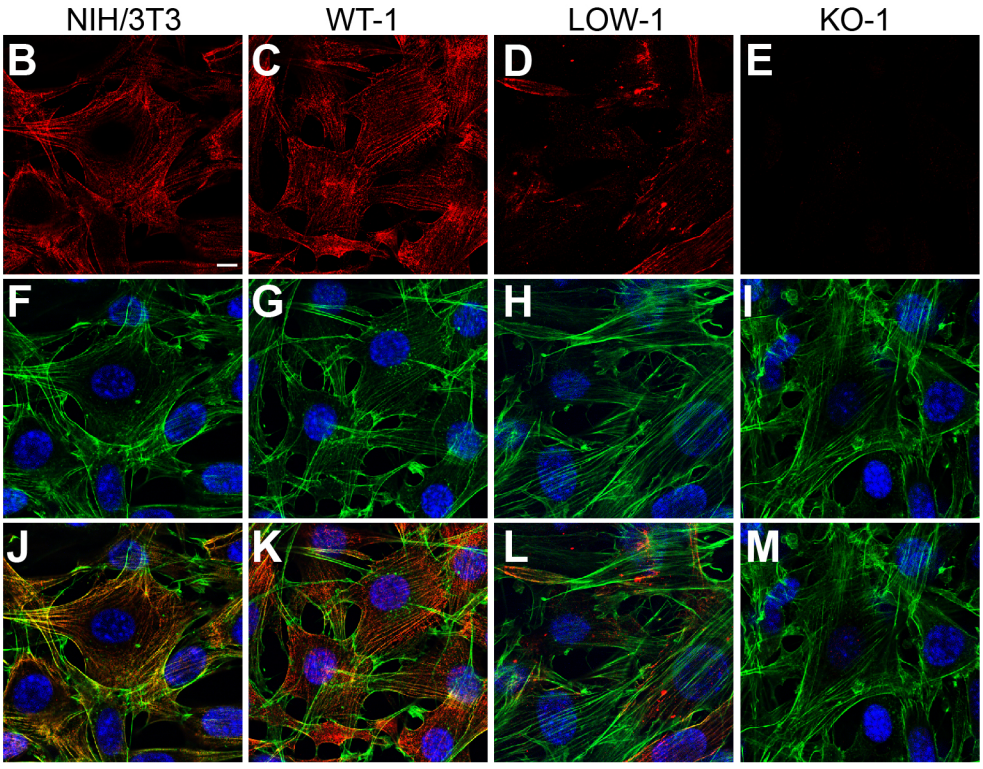
NIH/3T3
WT-1
LOW-1
KO-1
MYH10
PhaII/DAPI
Merge
B
C
D
E
F
G
H
I
J
K
L
M

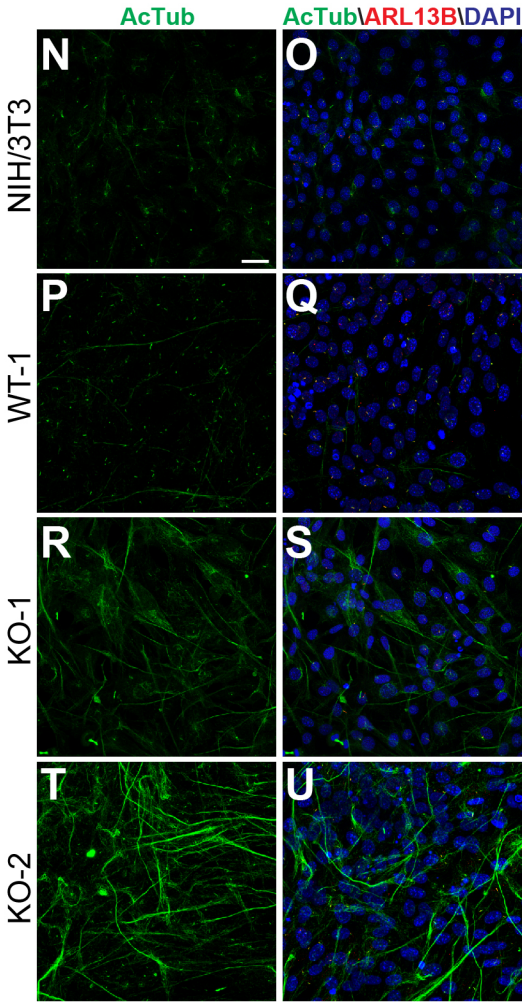
AcTub
AcTub\ARL13B\DAPI
NIH/3T3
WT-1
KO-1
KO-2
N
O
P
Q
R
S
T
U

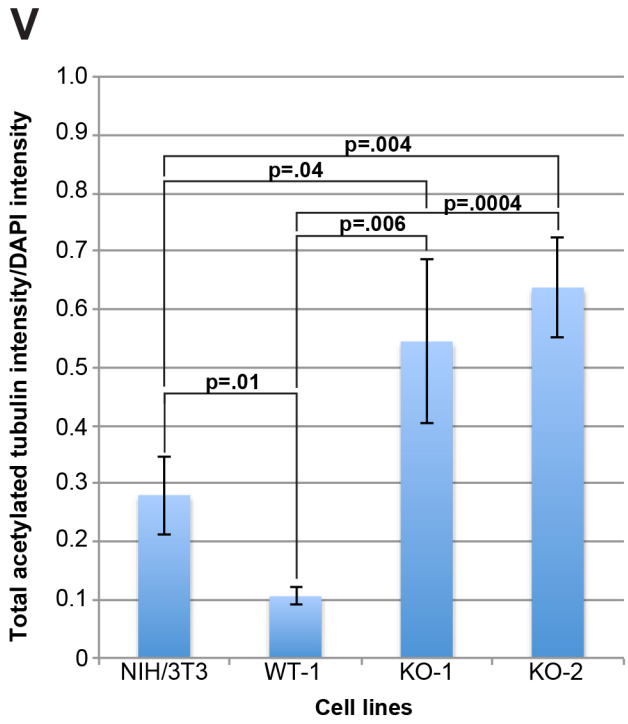
V
Total acetylated tubulin intensity/DAPI intensity
1.0
0.9
0.8
0.7
0.6
0.5
0.4
0.3
0.2
0.1
0
p=.004
p=.04
p=.0004
p=.006
p=.01
NIH/3T3
WT-1
KO-1
KO-2
Cell lines

Figure S7

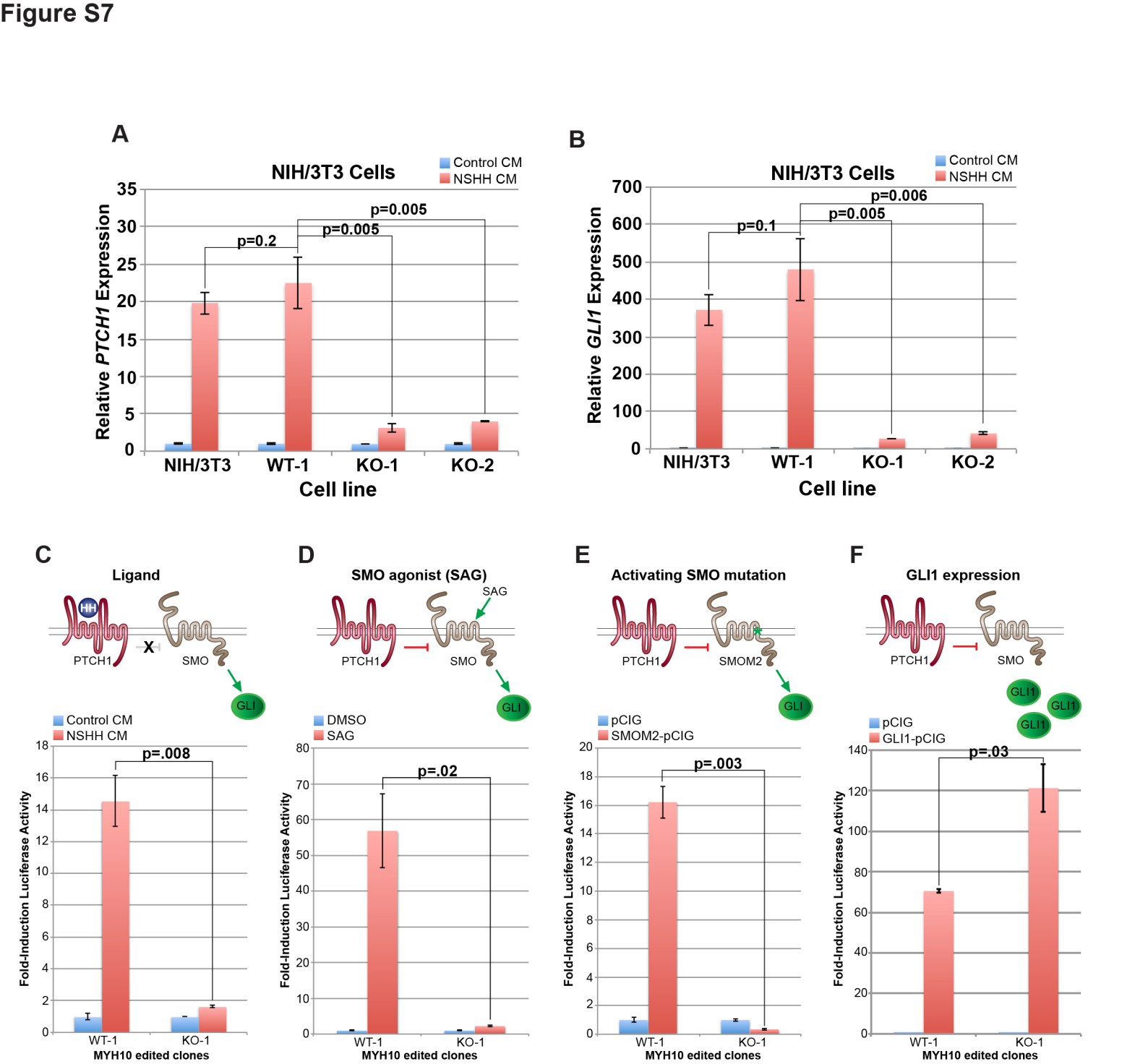
A
NIH/3T3 Cells
Control CM
NSHH CM
Relative PTCH1 Expression
p=0.2
p=0.005
p=0.005
NIH/3T3
WT-1
KO-1
KO-2
Cell line
B
NIH/3T3 Cells
Control CM
NSHH CM
Relative GLI1 Expression
p=0.1
p=0.005
p=0.006
NIH/3T3
WT-1
KO-1
KO-2
Cell line
C
Ligand
HH
PTCH1
SMO
GLI
Control CM
NSHH CM
Fold-Induction Luciferase Activity
p=.008
WT-1
KO-1
MYH10 edited clones
D
SMO agonist (SAG)
SAG
PTCH1
SMO
GLI
DMSO
SAG
Fold-Induction Luciferase Activity
p=.02
WT-1
KO-1
MYH10 edited clones
E
Activating SMO mutation
PTCH1
SMOM2
GLI
pCIG
SMOM2-pCIG
Fold-Induction Luciferase Activity
p=.003
WT-1
KO-1
MYH10 edited clones
F
GLI1 expression
PTCH1
SMO
GLI1
GLI1
GLI1
pCIG
GLI1-pCIG
Fold-Induction Luciferase Activity
p=.03
WT-1
KO-1
MYH10 edited clones

Figure S8

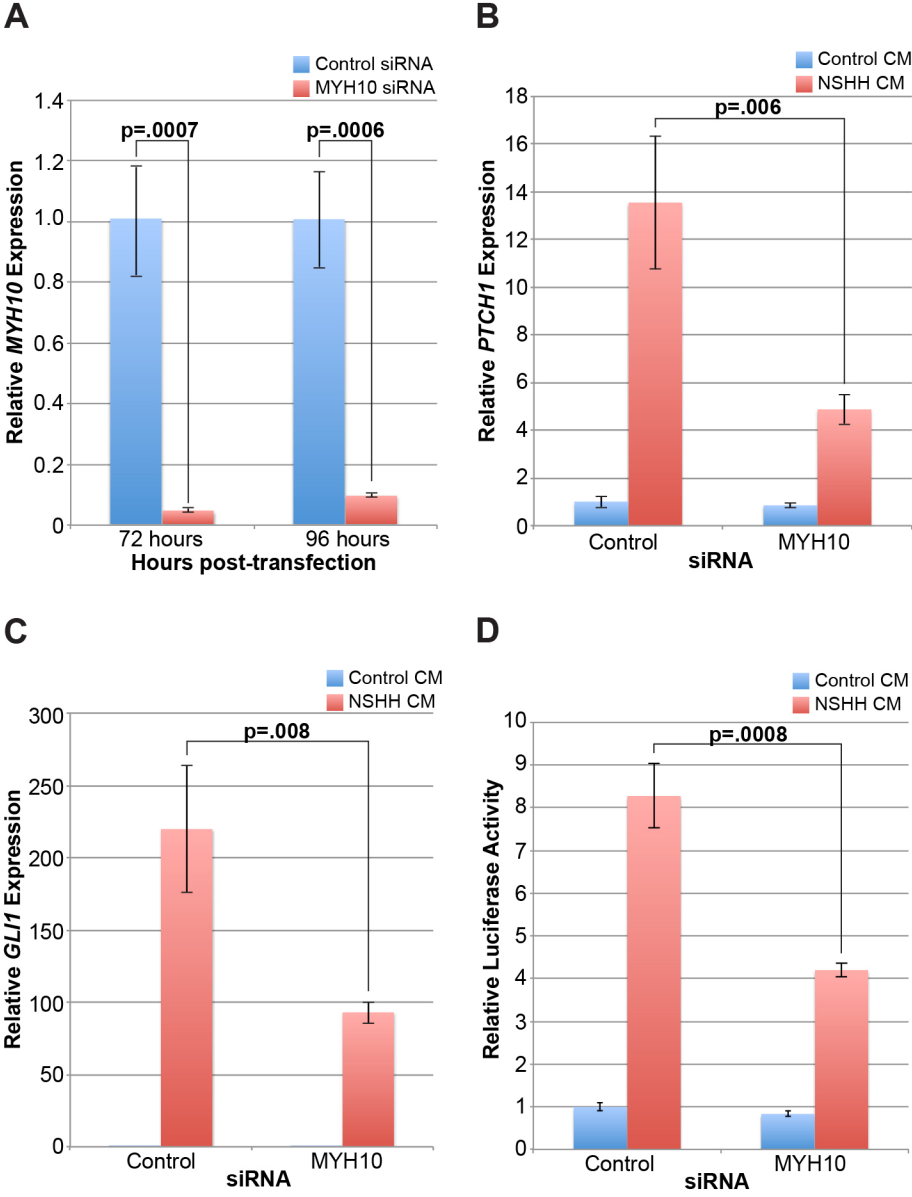
A
Control siRNA
MYH10 siRNA
Relative MYH10 Expression
1.4
1.2
1.0
0.8
0.6
0.4
0.2
0
p=.0007
p=.0006
72 hours
96 hours
Hours post-transfection
B
Control CM
NSHH CM
Relative PTCH1 Expression
18
16
14
12
10
8
6
4
2
0
p=.006
Control
MYH10
siRNA
C
Control CM
NSHH CM
Relative GLI1 Expression
300
250
200
150
100
50
0
p=.008
Control
MYH10
siRNA
D
Control CM
NSHH CM
Relative Luciferase Activity
10
9
8
7
6
5
4
3
2
1
0
p=.0008
Control
MYH10
siRNA

Figure S9

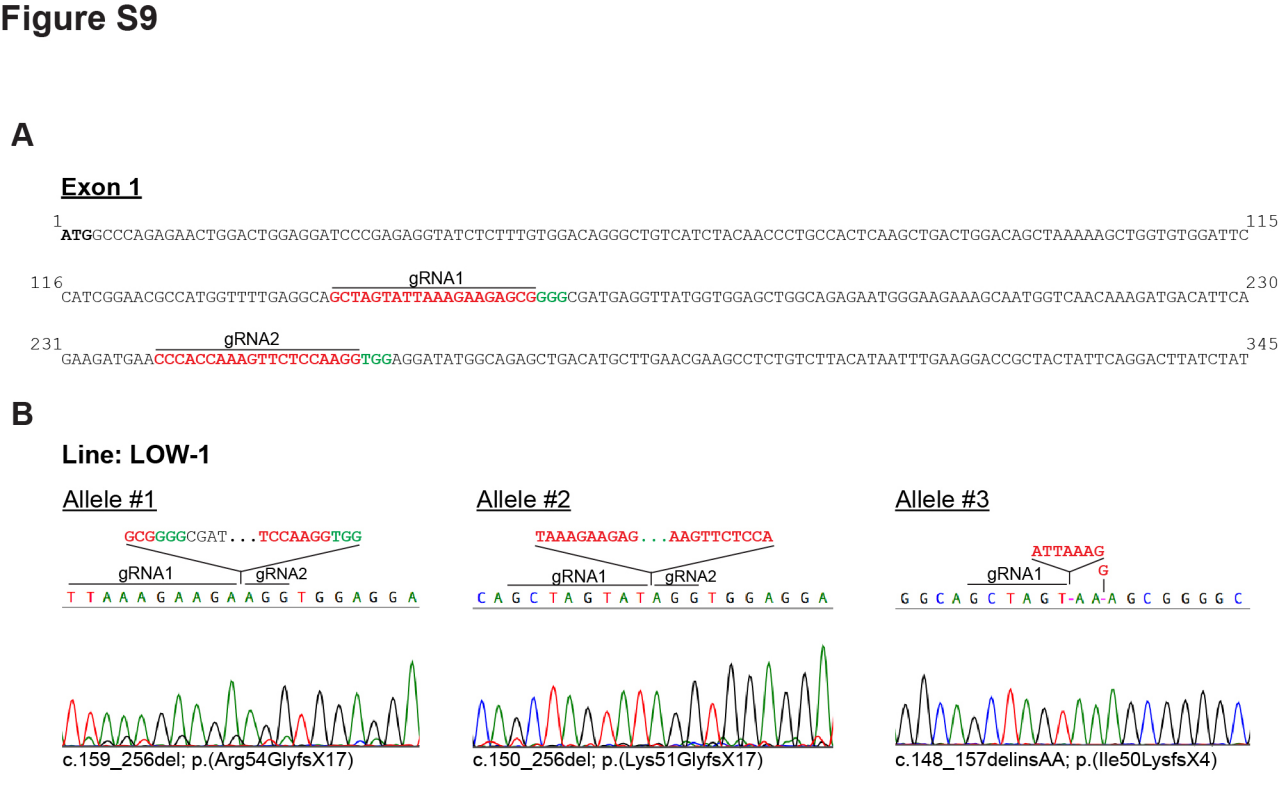
A
Exon 1
1
ATGGCCCAGAGAACTGGACTGGAGGATCCCGAGAGGTATCTCTTTGTGGACAGGGCTGTCATCTACAACCCTGCCACTCAAGCTGACTGGACAGCTAAAAAGCTGGTGTGGATTC
115
gRNA1
116
CATCGGAACGCCATGGTTTTGAGGCAGCTAGTATTAAAGAAGAGCGGGGCGATGAGGTTATGGTGGAGCTGGCAGAGAATGGGAAGAAAGCAATGGTCAACAAAGATGACATTCA
230
gRNA2
231
GAAGATGAACCCCACCAAAGTTCTCCAAGGTGGAGGATATGGCAGAGCTGACATGCTTGAACGAAGCCTCTGTCTTACATAATTTGAAGGACCGCTACTATTCAGGACTTATCTAT
345
B
Line: LOW-1
Allele #1
GCGGGGCGAT...TCCAAGGTGG
gRNA1
gRNA2
T T A A A G A A G A A G G T G G A G G A
c.159_256del; p.(Arg54GlyfsX17)
Allele #2
TAAAGAAGAG...AAGTTCTCCA
gRNA1
gRNA2
C A G C T A G T A T A G G T G G A G G A
c.150_256del; p.(Lys51GlyfsX17)
Allele #3
ATTAAAG
G
gRNA1
G G C A G C T A G T-A A-A G C G G G G C
c.148_157delinsAA; p.(Ile50LysfsX4)

Figure S10

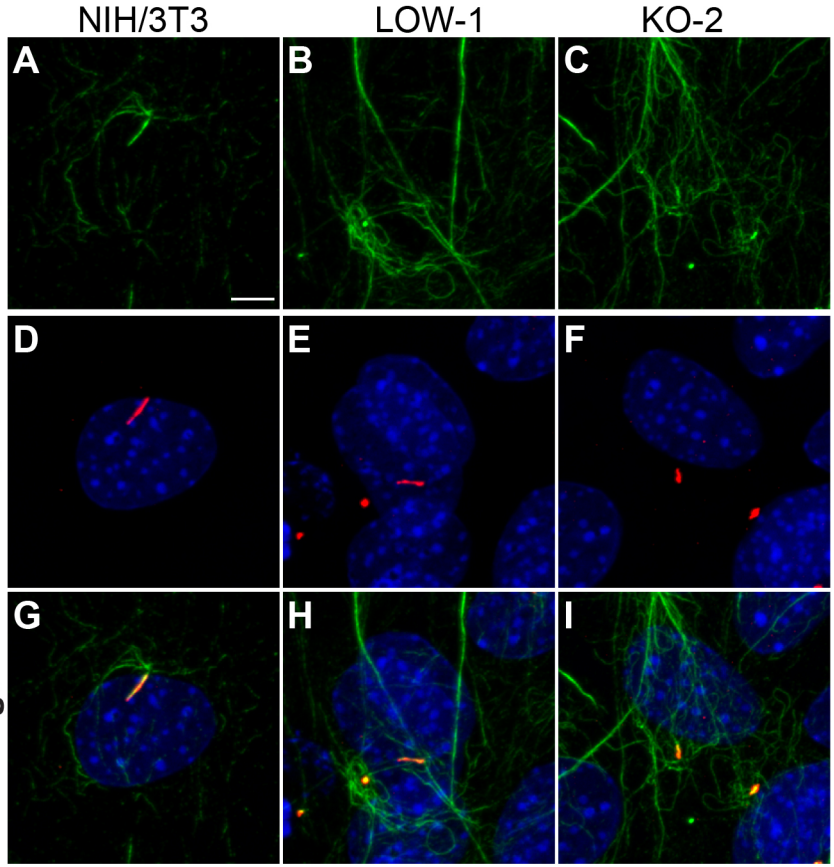
NIH/3T3
LOW-1
KO-2
A
B
C
D
E
F
G
H
I
AcTub
ARL13B\DAPI
Merge

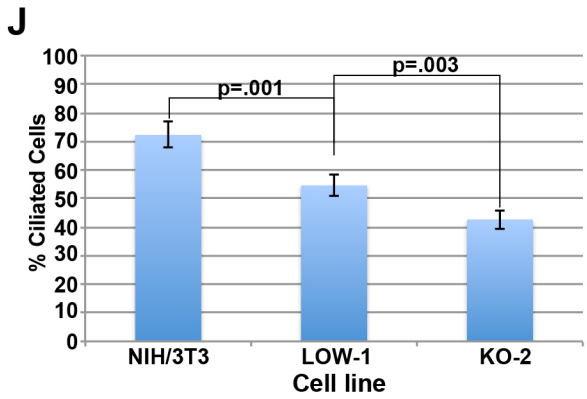
J
% Ciliated Cells
p=.001
p=.003
NIH/3T3
LOW-1
KO-2
Cell line

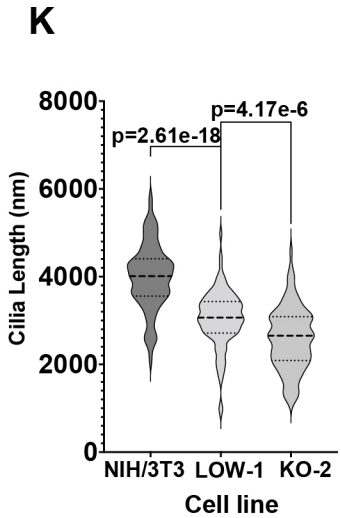
K
Cilia Length (nm)
p=2.61e-18
p=4.17e-6
NIH/3T3
LOW-1
KO-2
Cell line

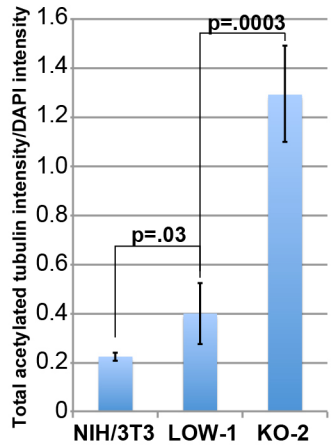
L
Total acetylated tubulin intensity/DAPI intensity
p=.0003
p=.03
NIH/3T3
LOW-1
KO-2

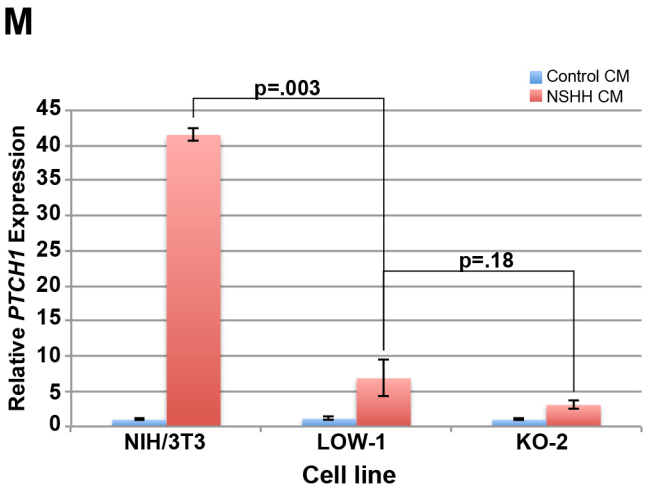
M
Control CM
NSHH CM
Relative PTCH1 Expression
p=.003
p=.18
NIH/3T3
LOW-1
KO-2
Cell line

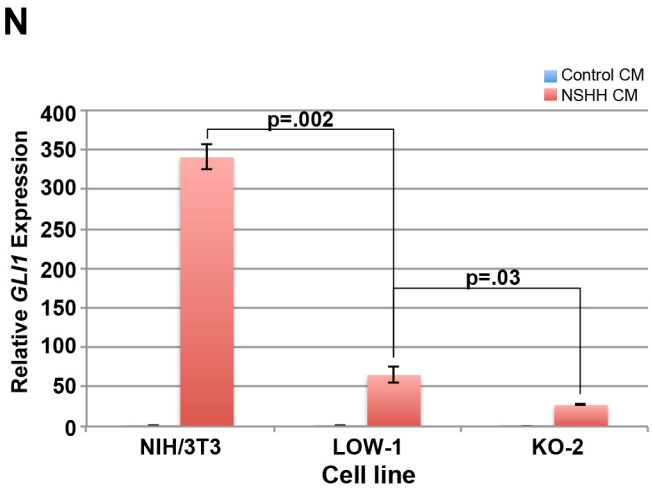
N
Control CM
NSHH CM
Relative GLI1 Expression
p=.002
p=.03
NIH/3T3
LOW-1
KO-2
Cell line

Figure S11

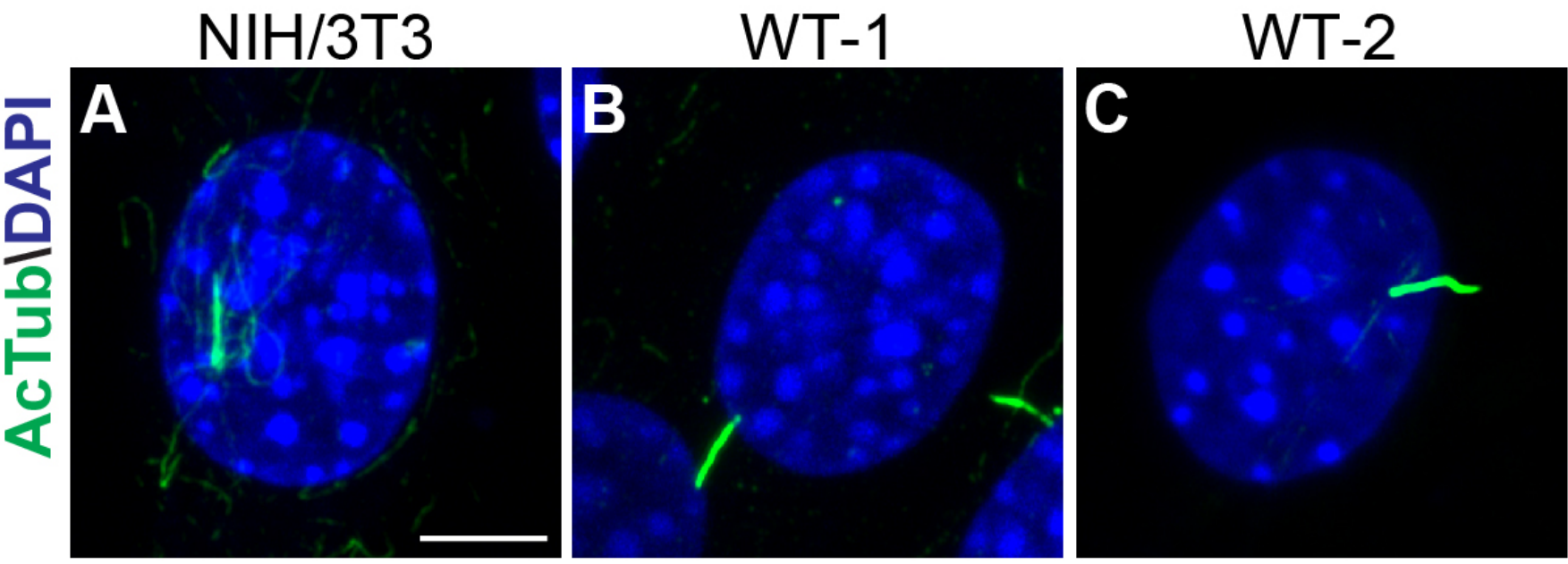
NIH/3T3
WT-1
WT-2
A
B
C
AcTub\DAPI

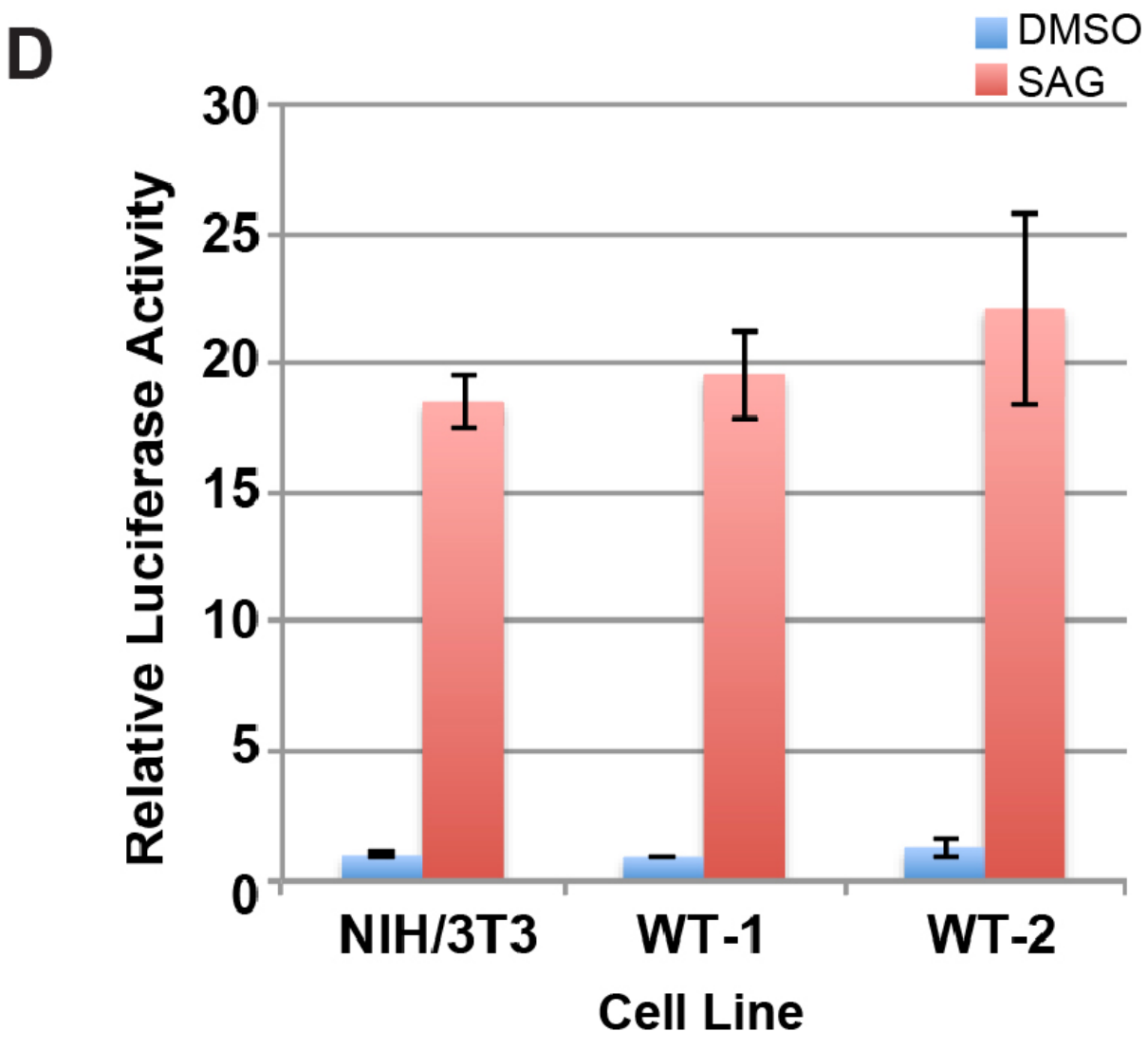
D
DMSO
SAG
Relative Luciferase Activity
30
25
20
15
10
5
0
NIH/3T3
WT-1
WT-2
Cell Line

Figure S12

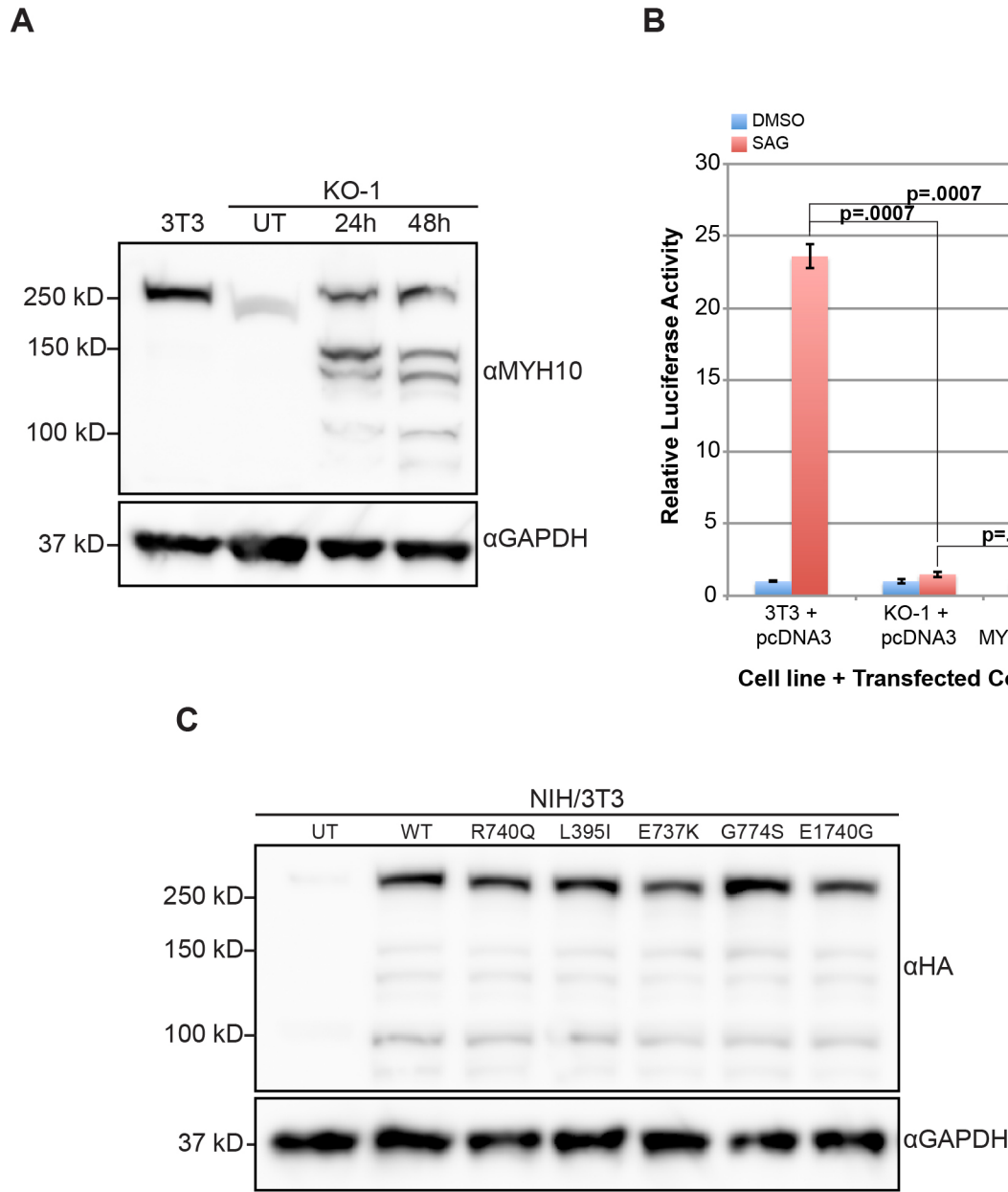
A
KO-1
3T3
UT
24h
48h
250 kD
150 kD
100 kD
αMYH10
37 kD
αGAPDH
B
DMSO
SAG
Relative Luciferase Activity
30
25
20
15
10
5
0
p=.0007
p=.0007
p=.2
3T3 + pcDNA3
KO-1 + pcDNA3
KO-1 + MYH10-pcDNA3
Cell line + Transfected Construct
C
NIH/3T3
UT
WT
R740Q
L395I
E737K
G774S
E1740G
250 kD
150 kD
100 kD
αHA
37 kD
αGAPDH

Figure S13

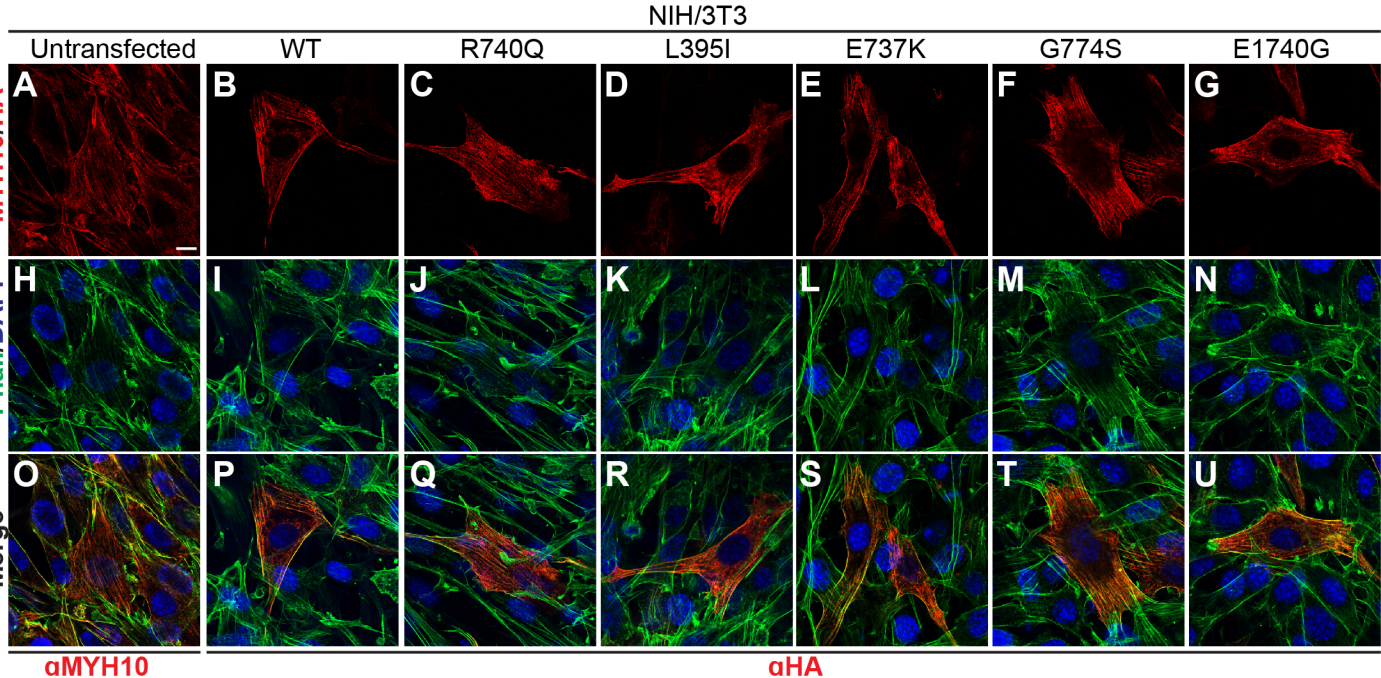
NIH/3T3
Untransfected
WT
R740Q
L395I
E737K
G774S
E1740G
MYH10/HA
Phall/DAPI
Merge
A
B
C
D
E
F
G
H
I
J
K
L
M
N
O
P
Q
R
S
T
U
αMYH10
αHA

Figure S14

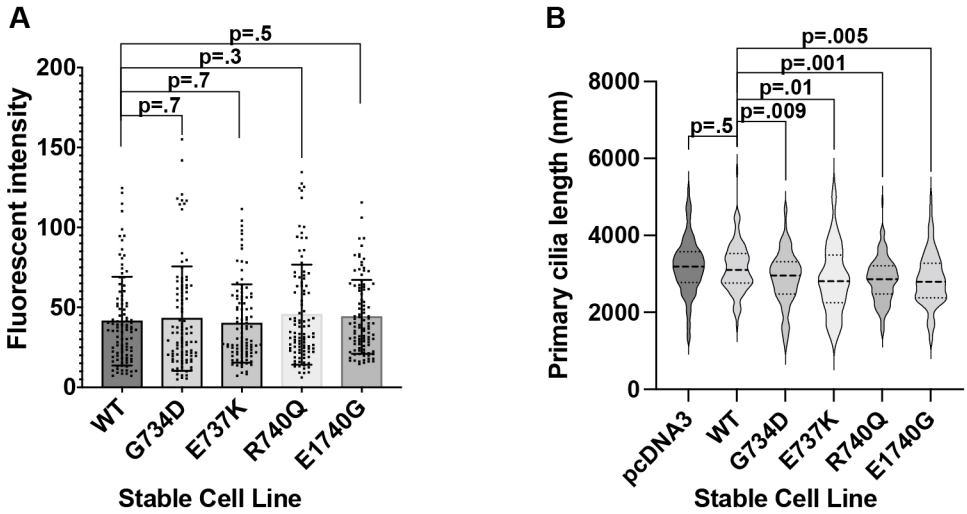
A
Fluorescent intensity
200
150
100
50
0
p=.5
p=.3
p=.7
p=.7
WT
G734D
E737K
R740Q
E1740G
Stable Cell Line
B
Primary cilia length (nm)
8000
6000
4000
2000
0
p=.005
p=.001
p=.01
p=.009
p=.5
pcDNA3
WT
G734D
E737K
R740Q
E1740G
Stable Cell Line

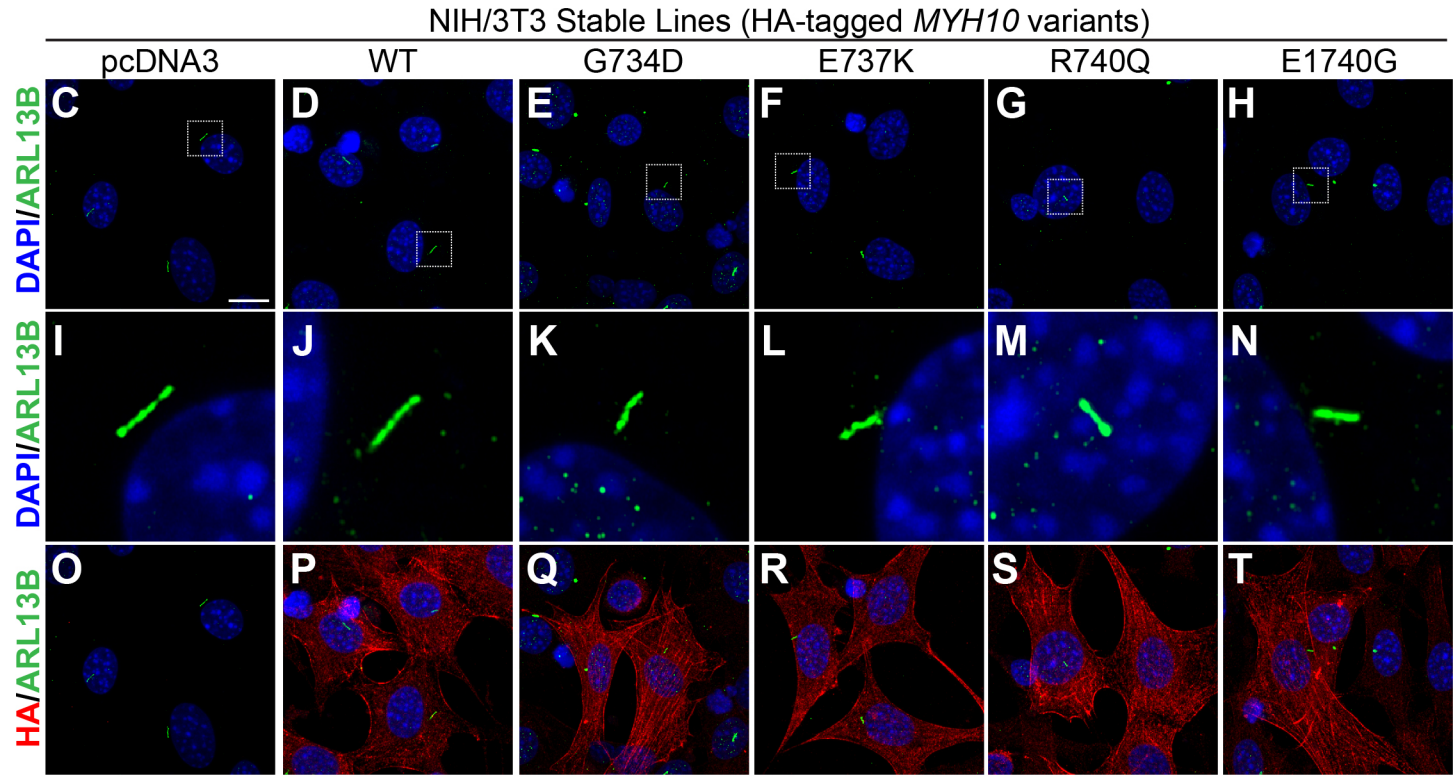
NIH/3T3 Stable Lines (HA-tagged MYH10 variants)
pcDNA3
WT
G734D
E737K
R740Q
E1740G
DAPI/ARL13B
DAPI/ARL13B
HA/ARL13B
C
D
E
F
G
H
I
J
K
L
M
N
O
P
Q
R
S
T

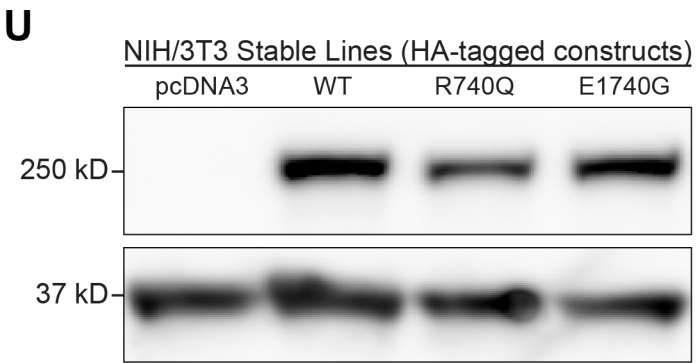
U
NIH/3T3 Stable Lines (HA-tagged constructs)
pcDNA3
WT
R740Q
E1740G
250 kD
37 kD

Figure S15

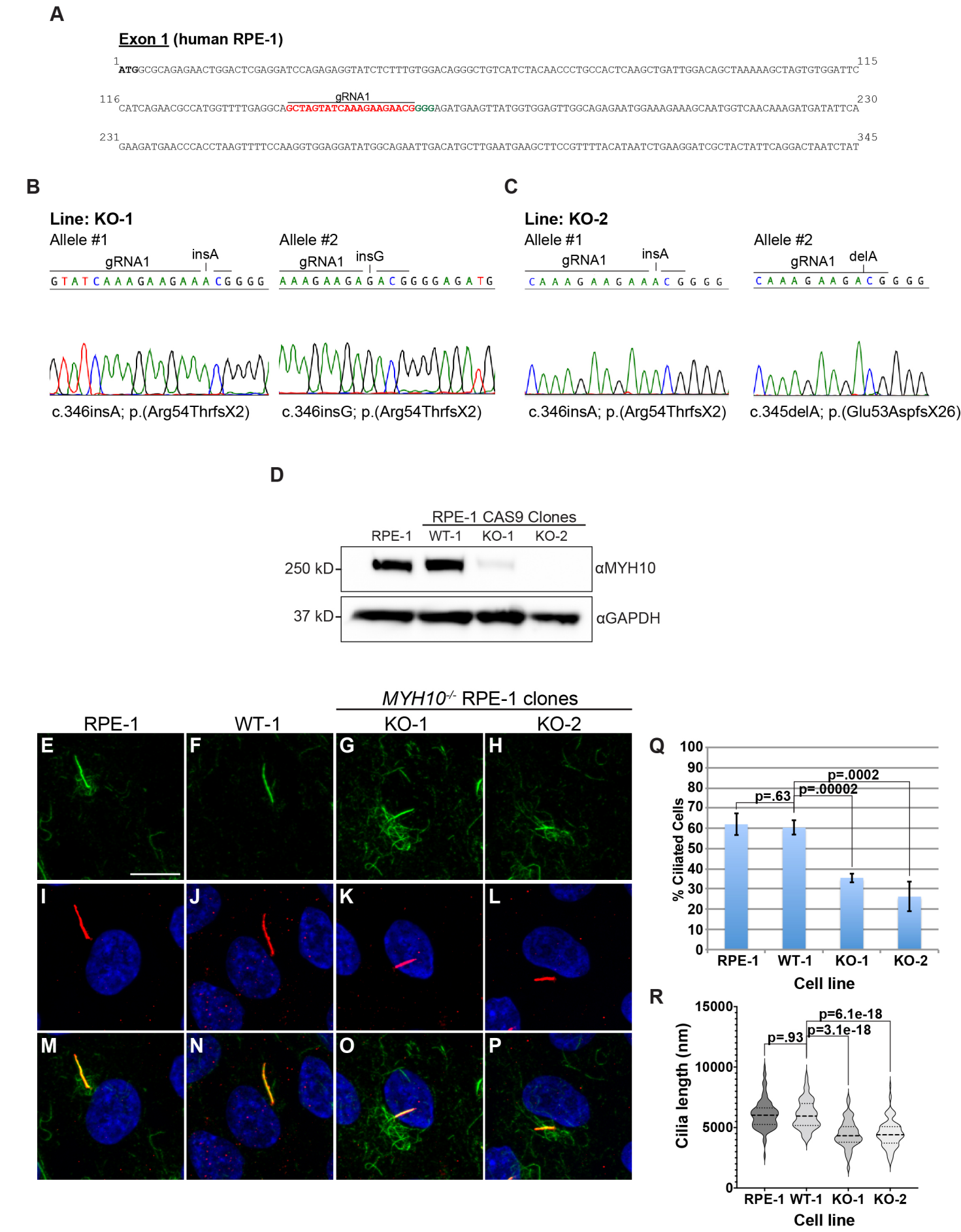
A
Exon 1 (human RPE-1)
1 ATGGCGCAGAGAACTGGACTCGAGGATCCAGAGAGGTATCTCTTTGTGGACAGGGCTGTCATCTACAACCCTGCCACTCAAGCTGATTGGACAGCTAAAAAGCTAGTGTGGATTC 115
gRNA1
116 CATCAGAACGCCATGGTTTTGAGGCAGCTAGTATCAAAGAAGAACGGGGAGATGAAGTTATGGTGGAGTTGGCAGAGAATGGAAAGAAAGCAATGGTCAACAAAGATGATATTCA 230
231 GAAGATGAACCCACCTAAGTTTTCCAAGGTGGAGGATATGGCAGAATTGACATGCTTGAATGAAGCTTCCGTTTTACATAATCTGAAGGATCGCTACTATTCAGGACTAATCTAT 345
B
Line: KO-1
Allele #1
gRNA1
insA
GTATCAAAGAAGAAACGGGG
Allele #2
gRNA1
insG
AAAGAAGAGACGGGGAGATG
c.346insA; p.(Arg54ThrfsX2)
c.346insG; p.(Arg54ThrfsX2)
C
Line: KO-2
Allele #1
gRNA1
insA
CAAAGAAGAAACGGGG
Allele #2
gRNA1
delA
CAAAGAAGACGGGG
c.346insA; p.(Arg54ThrfsX2)
c.345delA; p.(Glu53AspfsX26)
D
RPE-1 CAS9 Clones
RPE-1
WT-1
KO-1
KO-2
250 kD
αMYH10
37 kD
αGAPDH
MYH10-/- RPE-1 clones
RPE-1
WT-1
KO-1
KO-2
E
F
G
H
I
J
K
L
M
N
O
P
Q
% Ciliated Cells
100
90
80
70
60
50
40
30
20
10
0
p=.63
p=.00002
p=.0002
RPE-1
WT-1
KO-1
KO-2
Cell line
R
Cilia length (nm)
15000
10000
5000
0
p=.93
p=3.1e-18
p=6.1e-18
RPE-1
WT-1
KO-1
KO-2
Cell line